Application of Hierarchical Bayesian Modelling to long term avalanche forecasting

Eckert, Nicolas
Cemagref, UR ETGR
2 rue de la papeterie
38402 Saint Martin d'Hères, France
nicolas.eckert@cemagref.fr

Long term forecasting of snow avalanches

Snow avalanches occur frequently in many mountainous regions in winter. Hence, winter tourism is strongly susceptible to avalanche danger, whereas it is a vital and growing economic sector for mountain townships. Furthermore, because of the limited space available in these areas, exposition of settlements to snow avalanches has strongly increased during the last decades.

Casualties to back country skiers are relatively accepted by populations as soon as skiers evolve under their own responsibilities in risky terrain, knowing the daily risk level. On the contrary, casualties due to damages to infrastructures (roads and buildings, Figure 1) are no longer accepted. Indeed, whereas mountain inhabitants have had to accept a high level of risk during the past centuries, today's inhabitants, permanents and tourists, want the same safety level as everyone else in the country while they are staying in their houses or travelling on their roads.

It must be emphasised that no evacuation is possible after the avalanche has been released because of the extreme rapidity of the phenomenon. Preventive evacuations are sometimes attempted at the valley scale, but they can have catastrophic consequences if an event occurs when many people are on the road. As a consequence, a comprehensive alert phase to manage avalanche risk remains for the moment out of reach, and a simple message advising people to stay at home (possibly in cellars or in reinforced common buildings) can be considered as the best option for stake holders during critical situations. On the other hand, avalanche sites are well localised, with often historical testimonies available. This offers an appropriate basis for long term forecasting including the precise definition of hazard zones and the construction of permanent defence structures.

Figure 1: Building destroyed by a powder snow avalanche

20 January 1981, La Morte township, Isère, France (picture F. Valla/Cemagref).

Methods for evaluating high magnitude avalanches, and aim of this talk

A crucial step for proposing relevant long-term mitigation measures is the accurate definition of reference avalanches, i.e. of dangerous scenarios likely to occur. Following the example of flood mitigation, the existing guidelines generally use probabilistic definitions based on the return level. This is especially true since the catastrophic 1999 winter (SLF Davos, 2000) that has entrained a search for normalisation and equal exposition to risk at the European scale.

For evaluating high magnitude avalanches, direct use of standard extreme value theory (EVT, Coles 2001) is difficult, because of the strong dependency of the distribution of runout distances, the most critical variable, on path's geometry. Furthermore, for the structural design of buildings and defense structures, other variables such as impact pressure and flow depth must also be considered, and available series are usually too short and incomplete to fit multivariate extreme value models (e.g. Schlather, 2002) that corresponds to the engineers' needs.

Two traditional approaches exist. The first is based on simple statistical relations between runout distances and topographic descriptors of the avalanche path (e.g. Lied and Bakkehoi, 1980), with possible inclusion of concepts from EVT (Keylock, 2005). The second relies on deterministic propagation models based on the resolution of constitutive equations for the fluid in motion (e.g. Bartelt et al. 1999) associated with extreme snowfalls and tabulated friction parameters (Salm et al., 1990).

More recently, explicit combinations of a numerical propagation model with stochastic operators describing the variability of its inputs-outputs have emerged (e.g. Barbolini and Keylock, 2002; Meunier and Ancey, 2004). Main interests of such a "statistical-dynamical" approach is to take into account the topographic dependency of snow avalanche runout distances, and to impose the correlation structure by physical rules, so as to simulate the different marginal distributions of interest, including those for which no or little data is available, with a reasonable realism (Figure 2). Crucial problems are then model inference, and finding a reasonable compromise between precision of the description of the flow and computation times.

Figure 2: Principle of a statistical-dynamical approach

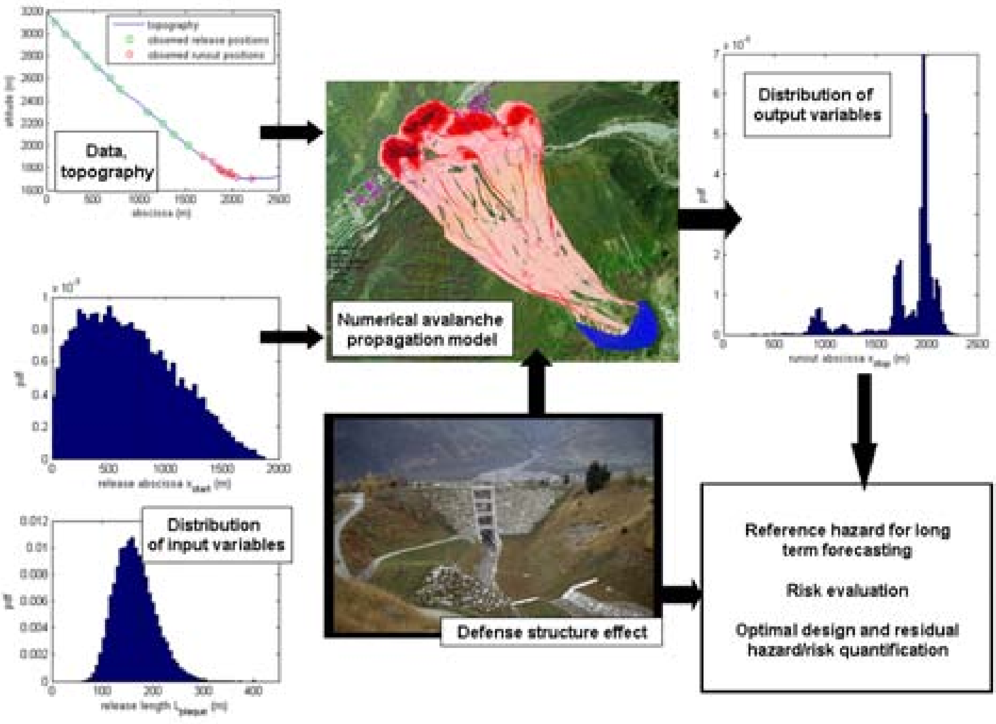

Avalanche numerical model from Naaim et al. (2004). Vertical avalanche dam, Rabuis, Switzerland (picture F. Rapin/Cemagref).

Bayesian methods are now seeing growing interest to overcome these difficulties (Ancey, 2005; Eckert et al., 2008a), and process the different variability/uncertainty sources in a consistent manner up to the engineering decision. The aim of this talk is to illustrate some of these developments, first for calibrating a numerical avalanche model, then for evaluating multivariate high magnitude avalanches, quantifying the effect of a defense structure on avalanche hazard and risk, and perform the optimal design of the defense structure by minimizing expected losses. The different aspects of the approach are illustrated with real case studies from the French Alps.

It must be noted that here hierarchical modelling is just used as a way of modelling variability from one avalanche to another on a given site under the strong assumption of time stationarity. Hence, spatio-temporal dependences to transfer information from one path to another and take into climate change effects are not considered. The spatio-temporal context is however a natural and fruitful extension of the framework worth to be mentioned (Eckert et al., 2007a; 2010a).

Runout distance, return period and reference scenarios

Formally, in a statistical-dynamical approach, the magnitude of each avalanche *i* is described by a couple of random vectors $\left(x_i, y_i\right)$. The x_i are the input variables corresponding to avalanche release and propagation: release area and altitude, snow depth, humidity and grain size, etc. The y_i are the output variables of interest in long term forecasting: runout distance, velocity and pressure fields. For evaluating annual probabilities and return periods, the avalanche occurrence rate is also necessary, so that the number of avalanche occurring each year a_t must also be modeled. Simulations allow reconstructing the joint distribution $p\left(x, y, a \middle| \hat{\theta}\right)$ by conditioning in agreement with the physics of the phenomenon:

$$p\left(x, y, a \middle| \hat{\theta}\right) = p\left(y \middle| a, x, \hat{\theta}\right) \times p\left(x \middle| a, \hat{\theta}\right) \times p\left(a \middle| \hat{\theta}\right) \quad (1)$$

The quantity $\hat{\theta}$ indicates that the obtained distribution depends on a vector of unknown quantities for which point estimates $\hat{\theta} = \left(\hat{\theta}_M, \hat{\theta}_F\right)$ are assumed to be available. θ_M and θ_F correspond to avalanche magnitude and frequency, respectively.

The return period $T_{x_{stop}}$ corresponding to the runout distance x_{stop} can be evaluated by combining the expected annual avalanche number $E\left[A \middle| \hat{\theta}_F\right]$ and $\hat{F}(x_{stop}) = P\left(X_{stop} \le x_{stop} \middle| \hat{\theta}_M\right)$, the estimated cumulative distribution function (cdf) of runout distances:

$$T_{x_{stop}} = \frac{1}{E\left[A \middle| \hat{\theta}_F\right] \times \left(1 - \hat{F}(x_{stop})\right)} \quad (2)$$

As an illustration, Figure 3 compares modelled and empirical return periods for a case study. The avalanche propagation model is a depth-averaged set of equation describing mass and momentum conservation. The stochastic magnitude model for the correlated quantitative characteristics that vary from one avalanche to another is described in Eckert et al. (2010b). It uses conditional distributions and mixed additive effects. The stochastic frequency model is a simple Poisson distribution independent from avalanche's magnitude, which leads to a pseudo Peak Over Threshold (POT) model where the threshold corresponds to avalanche release and the magnitude is given by the multivariate statistical-dynamical model. Model fit is reasonable.

The joint distribution of the exceedances $p\left(y\middle|\hat{\theta}_M, x_{stop} > x_{stop_T}\right)$ summarizes the characteristics of all avalanche events attaininf the abscissa x_{stop_T}. It can therefore be considered as the joint distribution of all the reference scenarios corresponding to the return period T. In the simulation set-up, it can simply be obtained by considering only the events for which the runout distance exceeds x_{stop_T}.

This partially counters the limitations of the return period for a multivariate hazard by giving the variation range that has to be considered for any return period. Figure 4 illustrates this point with marginal distributions of maximal velocity, Froude number, drag coefficient and impact pressure at a 10 year return period abscissa. The Froude number distribution allows quantifying the flow regime. Recent developments have been employed to compute impact pressures taking into account the rheology of snow, and, for instance, the increase of the drag coefficient relating velocity to impact pressure for slow dense flows (Naaim et al., 2008).

Figure 3: Return period for the runout distance on a two-dimensional topographical profile

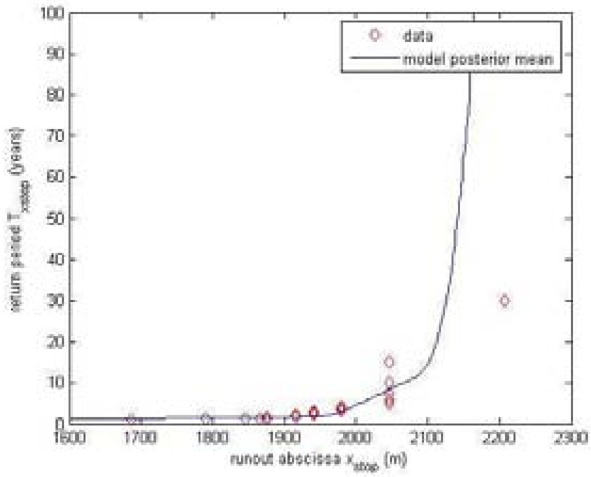

Avalanche model and case study from Eckert et al. (2010b).

Bayesian inference and prediction

To solve the crucial problem of the choice of the multivariate input distribution $p\left(x\middle|a,\hat{\theta}\right)$, the most natural solution is to estimate θ using the available data. For a non invertible model, even non explicit for its outputs, Bayesian inference using MCMC methods (e.g. Brooks, 1998; Gilks et al., 2001) is well adapted. In Bayes' theorem, $l\left(x,y,a\middle|\theta\right)$ is the probability of the data under the assumption that they are independent realizations of $p\left(x,y,a\middle|\theta\right)$, and $p(\theta)$ a *prior* distribution representing extra-data information about non observable quantities, which can be used to introduce expert knowledge into the analysis. $p(\theta|data)$ is the joint *posterior* distribution of model unknowns quantifying the remaining uncertainty given the limited data sample available:

$$p(\theta|data) \propto p(\theta) \times l(x, y, a|\theta) \quad (3)$$

It must be emphasized that here the generic notation $p(\theta|data)$ includes, in addition to model parameters, latent random variables: the quality of snow varying from one avalanche to another (friction parameters), and “true” simulated runout distances possibly different from observations. Hence, full inference about model parameters implies reconstructing these unobserved quantities, and integrating out over their distribution (Tanner, 1992). Implementation using a sequential Metropolis-Hastings algorithm and details to tune the algorithm in practice are given in Eckert et al. (2010b).

Figure 4: distribution of the output variables conditional to the exceedence of a 10 year return period abscissa

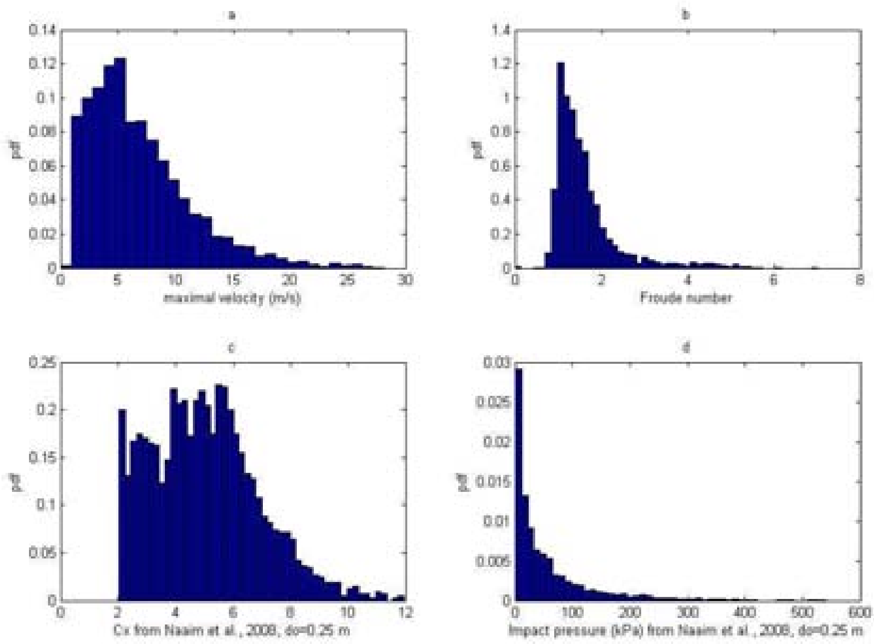

a) Maximal velocity, b) Froude number, c) Drag coefficient and d) Impact pressure computed following Naaim et al. (2008), for an obstacle typical diameter d_o=0.25 m. Avalanche model and case study from Eckert et al. (2010b)

Bayesian prediction is then an interesting option to evaluate the uncertainty associated with the chosen reference scenarios, mainly runout distances corresponding to high magnitude return periods (Eckert et al., 2007b). The predictive distribution $p(x_{stop_T}|data)$ for the runout distance x_{stop_T} corresponding to the return period T is obtained by averaging x_{stop_T} over the posterior distribution of magnitude and frequency unknowns. The quantile to be picked up is determined using the inverse cumulative distribution of runout distance $F_{x_{stop}}^{-1}$. Its dispersion depends on data quantity, and asymptotically it converges to the true point value x_{stop_T}:

$$p\left(x_{stop_T} \,|data\right) = \int F_{x_{stop}}^{-1}\left(1 - \frac{1}{T \times E\left[A|\theta_F\right]}\right) \times p\left(\theta_M, \theta_F \,|data\right) \times d\theta_M \times d\theta_F \quad (4)$$

As an illustration, Figure 5 presents the predictive distribution of the decennial and centennial abscissas for a case study. A sliding block model describing avalanche propagation is embedded within a stochastic model similar to the one discussed previously. The sharp peak in the decennial distribution shows the strong influence of topography, since it corresponds to the beginning of the valley bottom (the slope tends to zero), stopping a high proportion of avalanches. Furthermore, the strong dispersion and asymmetry of the centennial distribution shows well that uncertainty about model unknowns strongly affects the most extreme avalanches, and that values much higher that the best bet prediction must be envisaged.

Figure 5: Predictive distribution of runout distances

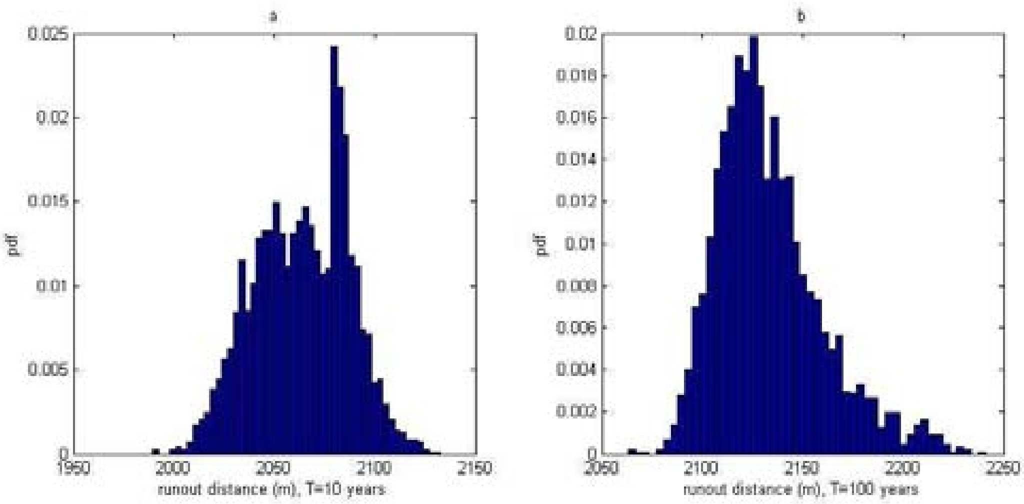

Abscissas corresponding to return periods of a) 10 years and b) 100 years. Avalanche model and case study from Eckert et al. (2009).

Risk evaluation for the design of a defense structure

The multivariate nature of snow avalanche hazard creates difficulties when trying to use legal thresholds such as the 100 year return period in practice. Cappabianca *et al.* (2008) list other important reasons that make hazard-oriented approaches insufficient to quantify avalanche risk. First, they do not consider the elements at risk, which makes it impossible to compare the level of exposure of different mountain communities to avalanche hazard, and of a given mountain community to different natural hazards such as debris flows, landslides, and rock falls. Second, they do not allow confronting different mitigation strategies such as land use planning policies, temporary evacuations or construction of permanent defence structures. This is clearly not adapted to the current context of limited public funds which requires testing different solutions and searching optimality.

To overcome these limitations, a quantitative risk evaluation combining a loss function and the hazard model is an interesting option, especially for the design of defense structures. However, optimal design methods remain for now little developed in the avalanche field, and simple cost-benefit analyses are generally preferred. Here the effect of including a dam in a stochastic avalanche model is studied, and the height of the dam h_d that maximizes the economical benefit of its construction is searched.

A loss function $C(h_d, y, a)$ depending on the dam height and on the avalanche hazard in the runout zone, where the elements at risk (people, buildings, traffic roads, etc.) are situated, must be specified. It depends on the number, nature and vulnerability (i.e., damage susceptibility to avalanche hazard) of these elements at risk. The choice is made to work in terms of total risk starting at the date of the dam construction rather than in annual values. This implies, under the assumption of stationarity of the avalanche phenomenon, introducing the actualization factor A for expressing the losses resulting from future damages in the current monetary unit. For simplicity, construction costs are taken into account using a linear additive form, and damages to the defense structure are neglected in first approximation. Furthermore, a single element at risk is considered, a building situated at a given abscissa of the runout zone, leading to the total loss function:

$$C(h_d, y, a) = C_o h_d + A \times E_d\left[a \middle| \theta_F, \theta_M\right] \times C_1(h_d, y) \quad (5),$$

where $C_1(h_d, y)$ is the loss resulting from the avalanche magnitude y with the dam height h_d, $E_d\left[a \middle| \theta_F, \theta_M\right]$ is the annual exceedence rate of the dam abscissa depending on avalanche frequency and magnitude models (censoring of the full POT model with a higher threshold), and C_o the linear construction cost.

For more complex systems at risk including several elements, total risk is simply the sum of the risk to each of the considered elements. Main limitation is then that one must be able to express all of the elements by the same unit. For instance, a critical point which is often debated is how to take human lives into account, and compare them to pieces of equipment. Similarly, difficulties also arise if one wants to consider the less tangible elements at risk and compare them to material values. Mathematical convenience is to follow insurance techniques and to express everything in the same monetary currency. Alternatively, all the computations can be carried out by considering only one kind of element at risk, for instance human lives or buildings, leading to a risk that has to be interpreted as an expected number of deaths or destroyed buildings.

Following Von Neuman and Morgenstern (1953)'s seminal work in economics, the classical risk R_C is the expected damage, depending on the decision variable, on the chosen loss function, and on the avalanche magnitude and frequency models for which point estimates $\left(\hat{\theta}_M, \hat{\theta}_F\right)$ are assumed to be known:

$$R_C\left(h_d, \hat{\theta}_M, \hat{\theta}_F\right) = C_o h_d + A \times E_d\left[a \middle| \hat{\theta}_M, \hat{\theta}_F\right] \times \int C_1(h_d, y) \times p\left(y \middle| \hat{\theta}_M\right) \times dy \quad (6)$$

Finally, to evaluate $C_1(h_d, y)$, the influence of the dam on relatively rapid avalanche flows is expressed as a linear relation between the runout distance reduction and the ratio between the dam height, h_d, and the depth of the avalanche flow without the dam (Faug *et al.*, 2008). With a simple exponential distribution of avalanche runouts and a 0-1 "step" vulnerability function leading to a total destruction of the building as soon as it is attained, this all leads to an easy quantification of the residual hazard and of the residual risk as functions of the dam height and of the building position in the runout zone (Figure 6).

Seen rather as a function of h_d, the classical risk can be minimized to determine the dam height that maximizes the benefit from the dam construction:

$$h_C^* = \text{Arg}\min_{h_d}\left(R_C\left(h_d, \hat{\theta}_M, \hat{\theta}_F\right)\right) \quad (7)$$

Figure 7 goes back to a multivariate numerical avalanche model. The vulnerability formulation used is derived from those available in the literature, relating the damage to the building to impact pressure in a simple semi-empirical way (Barbolini et al., 2004). Risk evaluation is performed numerically for each dam height by Monte Carlo integration for a building situated at a 100 year return period abscissa. The obtained risk function is nicely shaped, with a clear optimal height h_C^*=5m corresponding to the minimization of expected losses. For dam heights lower than the optimum, the expected losses decrease when the dam height increases. For higher dams, the expected losses increase again, indicating that the additional protective effect no longer compensates the additional construction cost.

Figure 6: Residual hazard and residual risk after a dam construction

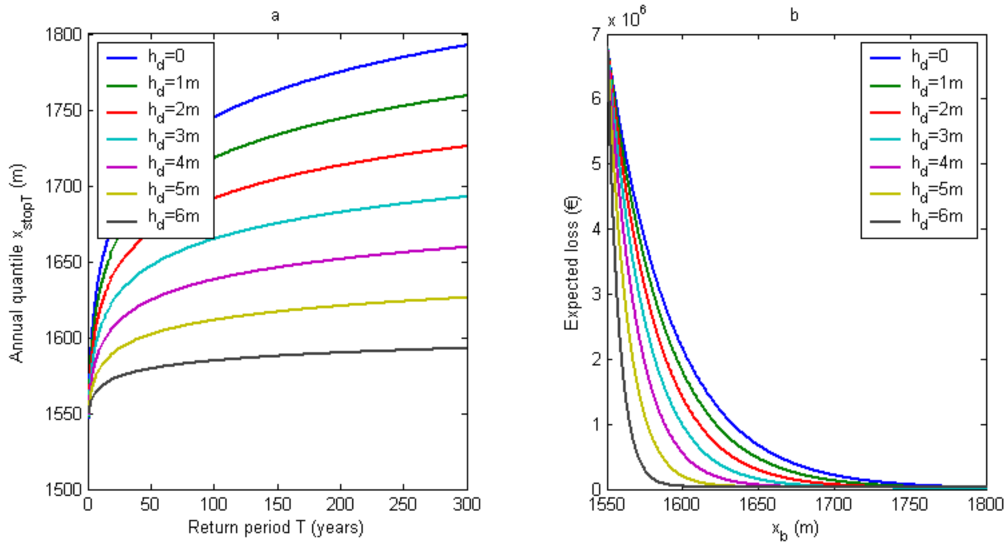

a) Annual quantile x_{stop_T} for different dam heights h_d. b) Residual risk representing the total expected loss as a function of the abscissa position of a single building x_b for different dam heights. Analytical model and case study from Eckert et al. (2008b).

Bayesian optimal design

Separating decision from model inference may however bias the decision in an undesirable way, because classical calibration to obtain point estimates for (θ_F, θ_M) is generally performed by minimization of a variance criterion, e.g. of a symmetrical quadratic function, whereas, in the context of natural hazards, the penalty to be applied for the decision is clearly asymmetrical. As an obvious example, the total losses increase much more strongly if an avalanche dam height is overestimated by a given value than if it is underestimated by the same amount. Again, this problem is fairly addressed within the Bayesian framework by averaging over the *posterior* distribution, leading to the Bayesian risk:

$$R_B(h_d) = \int R_C(h_d, \theta_M, \theta_F) \times p(\theta_M, \theta_F | data) \times d\theta_M \times d\theta_F \quad (8)$$

From a practical point of view $R_B(h_d)$ is, a function of h_d only instead of being a function of model parameters also, making the search of the optimal height $h_B^* = \text{Arg}\min_{h_d}(R_B(h_d))$ that minimises the expected losses easier. From a more theoretical point of view, it can be shown that h_B^* has suitable properties with regards to the statistical risk, see below.

In the illustrative example, the Bayesian optimal height is 20% higher (6m versus 5m) than the classical one, and the benefit expected from the construction of the optimal dam is 54% higher when the Bayesian computation is used (41 465 €) than when the classical computation is used (28 863). The absolute difference $R_B(h_B^*) - R(h^*)$=14 602 € can be interpreted as the expected opportunity loss for the Bayesian decision rule against the minimization of expected losses under the classical paradigm. It is attributable to the limited sample size of avalanche runouts on the case study. In other words this is the value quantifying what the decision maker should be ready to pay to obtain perfect information with full confidence, *i.e.* to fund an exhaustive data collection protocol. Optimal properties of Bayes' decision rules grant that other decisional procedures would yield a lower expected profit for the decision maker (Wald, 1950). Note also that the systematic difference between the Bayesian and classical optimal heights increases from 5% to 250% for return periods of the building abscissa ranging from 10 to 1 000 years (not shown). Taking estimation error into account therefore affects, in particular, the optimal design of a defence structure protecting buildings threatened only by the most extreme events, a crucial point in an engineering context.

Figure 7: Classical and Bayesian optimal design of an avalanche dam.

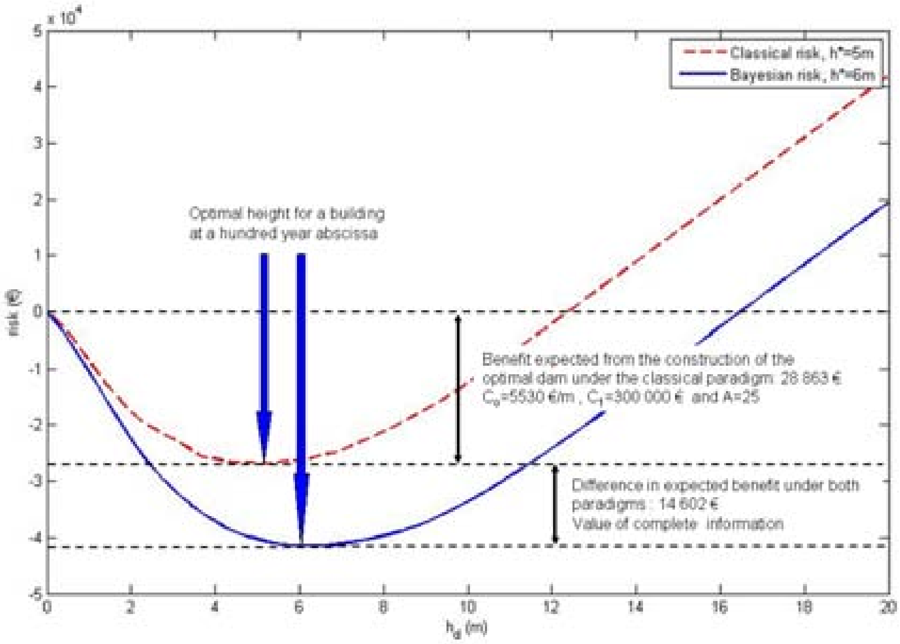

Risk model and case study from Eckert et al. (2009). Risk represents the opposite of the expected benefit as a function of the dam height, i.e. the baseline risk is subtracted from the expected loss for each dam height. A single building situated at a 100-year abscissa position without dam is considered.

Acknowledgements

This talk contains ideas of many people, including E. Parent (AgroParisTech Paris, France), M. Naaim, D. Richard and T. Faug (Cemagref Grenoble, France), C.J. Keylock (University of Sheffield, UK). An important part of the work has been done within the framework of the MOPERA project funded by the French National Research Agency (ANR-09-RISK-007-01).

REFERENCES

Ancey, C. (2005). Monte Carlo calibration of avalanches described as Coulomb fluid flows. Philosophical Transactions of the Royal Society of London A. 363. pp 1529-1550.

Barbolini, M., Keylock, C.J. (2002). A new method for avalanche hazard mapping using a combination of statistical and deterministic models. Natural Hazard and Earth System Sciences. 2. pp 239-245.

Barbolini, M., Cappabianca, F., Sailer, R. (2004). Empirical estimate of vulnerability relations for use in snow avalanche risk assessment. Atti del convegno Risk Analysis 2004, pp 533-542, 27-29 Settembre, Rodi, Grecia. Ed. C. A. Brebbia.

Bartelt, P., Salm, B., Gruber, U. (1999). Calculating dense-snow avalanche runout using a Voellmy-fluid model with active/passive longitudinal straining. Journal of Glaciology. 45. pp 242-254.

Brooks, S. P. (1998). Markov Chain Monte Carlo Method and its application. The Statistician. Vol 47, 1. pp 69-100.

Cappabianca, F., Barbolini, M., Natale, L. (2008). Snow avalanche risk assessment and mapping: A new method based on a combination of statistical analysis, avalanche dynamics simulation and empirically-based vulnerability relations integrated in a GIS platform. Cold Regions Science and Technology. 54. pp 193–205.

Coles, S. (2001). An introduction to statistical modelling of extreme values. Springer ed. 208p.

Eckert, N., Parent, E., Belanger, L. Garcia, S. (2007a). Hierarchical modelling for spatial analysis of the number of avalanche occurrences at the scale of the township. Cold Regions Science and Technology 50. pp 97-112.

Eckert, N., Parent, E., Richard, D. (2007b). Revisiting statistical–topographical methods for avalanche predetermination: Bayesian modelling for runout distance predictive distribution. Cold Regions Science and Technology. 49. pp 88-107.

Eckert, N., Parent, E., Naaim, M., Richard, D. (2008a) Bayesian stochastic modelling for avalanche predetermination: from a general system framework to return period computations. Stochastic Environmental Research and Risk Assessment. 22. pp 185-206.

Eckert, N., Parent, E., Faug, T., Naaim, M. (2008b). Optimal design under uncertainty of a passive defense structure against snow avalanches: from a general Bayesian framework to a simple analytical model. Natural Hazards and Earth System Sciences. 8. pp 1067-1081.

Eckert, N., Parent, E., Faug, T., Naaim, M. (2009). Bayesian optimal design of an avalanche dam using a multivariate numerical avalanche model. Stochastic Environmental Research and Risk Assessment. 23. pp 1123-1141.

Eckert, N., Parent, E., Kies, R., Baya, H. (2010a). A spatio-temporal modelling framework for assessing the fluctuations of avalanche occurrence resulting from climate change: application to 60 years of data in the northern French Alps. Climatic Change. Vol. 101, N° 3-4. pp 515-553.

Eckert, N., Naaim, M., Parent, E. (2010b). Long-term avalanche hazard assessment with a Bayesian depth-averaged propagation model. Journal of Glaciology. Vol. 56, N° 198. pp 563-586.

Faug, T., Gauer P., Lied K., Naaim, M. (2008). Overrun length of avalanches overtopping catching dams: Cross-comparison of small-scale laboratory experiments and observations from full-scale avalanches. Journal of Geophysical Research 113. F03009, doi:10.1029/2007JF000854.

Gilks, W. R., Richardson, S., Spiegelhalter, D. J. (2001). Markov Chain Monte Carlo in Practice. Chapman & Hall ed. 486 p.

Keylock, C. J. (2005). An alternative form for the statistical distribution of extreme avalanche runout distances. Cold Regions Science and Technology. 42. pp 185-193.

Lied, K., Bakkehoi, S. (1980). Empirical calculations of snow-avalanche run-out distances based on topographic parameters. Journal of Glaciology. 26 (94). pp 165-176.

Meunier, M., Ancey, C. (2004). Towards a conceptual approach to predetermining high-return-period avalanche run-out distances. Journal of Glaciology. 50-169. pp 268-278.

Naaim, M., Naaim-Bouvet, F., Faug, T., Bouchet, A. (2004). Dense snow avalanche modelling: flow, erosion, deposition and obstacle effects. Cold Regions Science and Technology. 39. pp 193-204.

Naaim, M., Faug, T., Thibert, E., Eckert, N., Chambon, G., Naaim, F. (2008). Snow avalanche pressure on obstacles. Proceedings of the International Snow Science Workshop. Whistler. Canada. September 21st-28th 2008.

Salm, B. Burkard, A., Gubler, H.U. (1990). Calcul des avalanches : une méthode pour le praticien avec des exemples. Communication de l'institut fédéral suisse pour l'étude de la neige et des avalanches, C. Ancey traducteur. 38p.

Schlather, M. (2002). Models for stationary max-stable random fields. Extremes. 5. pp 33–44.

SLF Davos (2000). Der Lawinenwinter 1999. Ereignisanlyse. 588 p.

Tanner, M. H. (1992). Tools for Statistical Inference: Observed Data and Data Augmentation Methods. Springer-Verlag ed.

Von Neumann, J., Morgenstern, O. (1953). Theory of Games and Economic Behaviour. New Jersey, USA. Princeton University Press.

Wald, A. (1950). Statistical Decision Functions. Wiley ed. 179p.